Exploring Overpressure Events in Compartment Fires

Charles Fleischmann (iD)*, *Daniel Madrzykowski and Nicholas Dow, UL Firefighter Safety Research Institute, Columbia, MD, USA*

Abstract. For more than a century, smoke explosions have been documented in the fire research literature. Yet even with this long history, smoke explosions have received very little attention in the fire research community. The few review articles on unexplained explosions (overpressure events) have adopted the conventional names of smoke explosions, backdraft, smoke gas explosions or rapid fire progression. Anecdotal evidence from firefighters have shown a number of overpressure events that cannot be explained as a gas leak or flammable liquids ignition. In this study, experiments were conducted in a plywood lined compartment with a timber crib as a sustained fire source and the ignition source. The compartment had a single vent that was open for the entire time. After an extended period of burning, the flames detached from the crib, traveled around the compartment, and finally self-extinguished. Sometime after the flames self-extinguished, the compartment erupted in flames culminating in a large horizontal flame projecting more than 2 m from the vent opening. In this study, a consistent cycle that leads to an overpressure event has been identified. A total of 29 overpressure events were created in 13 experiments with many experiments experiencing multiple overpressure events. Gas species, compartment temperatures, vent velocities, and compartment pressure were all recorded during the experiments. Conditions in the compartment immediately prior to the overpressure event are reported. Having demonstrated that an overpressure event within a combustible compartment can be reproduced, future research is recommended to better quantify the conditions leading to an overpressure event.

Keywords: Overpressure event, Smoke explosion, Backdraft, Compartment fires, Fire dynamics

1. Introduction

A review of the fire service literature shows that as far back as 1914 Steward [1] identified overpressure events (OPE) in accidental structure fires. Steward's explanation for an explosion in a smoke-filled compartment was the incomplete combustion of cellulosic material producing carbon particles and gases present in the smoke in a similar manner to dust explosions. Steward referred to such events as smoke explosions but noted that such events were also referred to as "back draughts" or "hot air explosions". Subsequent reviews by Croft [2] and later by Chitty [3] focused on fire incidents involving unexplained explosions that resulted

---

* Correspondence should be addressed to: Charles Fleischmann, E-mail: charley.fleischmann@ul.org

in firefighter injuries and fatalities. Incidents where the explosion could be readily explained, such as open chemical plant fires, were not included in the reviews. In Croft's study, fires involving such explosions are referred to as backdrafts, smoke explosions, or hot air explosions. Croft reviewed 2700 fire journals from 1907 to 1976 in which he identified 127 fires where firefighters were subjected to explosions. The review covered mostly the US and UK and was limited to incidents where there was enough information reported in the fire journals for inclusion in the review and analysis. The fires were divided into three categories of fires involving explosions: smoldering fire, developing fires, and developing fires with secondary explosions. There were 52 smoldering fires that resulted in 30 fatalities and 86 injuries. In 74% of the smoldering fires involving explosions, cellulosic fuels were identified as the material causing the explosion. This finding clearly demonstrates the importance of cellulosic fuels in these poorly understood explosions.

The most recent review into US fire service fatalities, 2009–2018, conducted by Fahy [4], showed that there were 101 firefighter fatalities where the firefighters were operating inside and on the structure. Of these fatalities, 20 firefighters were caught or trapped by "fire progression" that includes backdraft, flashover, and explosions. Unfortunately, it is not possible to further refine the term "fire progressions". As a result of these fatalities, Fahy emphasized the importance of firefighters understanding these phenomena:

> Firefighters must recognize the danger signs—fires burning in basements and attics indicating the potential for structural collapse, hot smoke and rolling flames at the ceiling indicating a potential flashover, and heavy, dirty smoke pushing through cracks in walls and at eaves indicating a potential backdraft, etc.—and respect them.

Unfortunately, in many fire service publications, backdraft and smoke explosions are used synonymously. This includes the preeminent standard on fire investigation, NFPA 921, that defines a smoke explosion by referring the reader to the definition for backdraft [5]. Use of the terms backdraft and smoke explosion in the fire service have also become comingled.

Previous research has attempted to define the difference between backdraft and smoke explosions where the defining feature is a change in ventilation conditions [6]. Most of the research on backdrafts has focused on the scenario of a fire inside a closed room where the fire is severely limited by the ventilation causing the production of large amounts of excess pyrolyzates (unburned fuel). When a vent becomes available, such as a firefighter opening a door, cold, oxygen rich air enters the compartment, while simultaneously allowing the hot (fuel rich) compartment gases to exit the compartment. This results in a buoyancy driven exchange flow referred to as a gravity current that mixes the fuel rich gases with the oxygen rich air. If this mixture of gases is within the flammable range and there is an ignition source present, a backdraft occurs, often culminating in a large fireball outside the fire compartment. The gravity current can be problematic to firefighters as it may allow them to enter the compartment shortly before the ignition of the event. Subsequent research has confirmed the time delay caused by the gravity current and have confirmed the scenario experimentally using different

fuels [7–13]. In these studies, the researchers have relied on a single fire source in a non-combustible compartment.

In contrast to backdrafts, smoke explosions are believed to occur without any change in the ventilation—when a fire in a closed room simply erupts with explosive force. Previous research on smoke explosions has focused on fires in noncombustible compartments with small ventilations openings and a timber crib as the only fuel source [14–16]. In these experiments, the fire starts as an initial flaming fire that transitions into a detached flaming fire that travels around the compartment before the flame self-extinguishes and the crib enters into a smoldering phase. The fire may oscillate between detached flaming and smoldering states before erupting into a smoke explosion, discharging flame outside the vents. In some experiments, multiple smoke explosions may occur over a 1–2 h experiment.

Given the ever-increasing availability of video recording devices, more and more overpressure events (OPE) are being informally documented. The most common question about these events caught on camera is: was this a backdraft or smoke explosion?

On December 13, 2018, the FDNY responded to a fire that involved several stores that were part of a building occupying one side of a city block. Firefighting operations had been underway for more than 45 min. Doors and some windows on the street level were open, portions of the roof were vented, and water was being applied to multiple areas of the building. Smoke was flowing out of the roof vents, open doors, and windows. With no identifiable change in ventilation, smoke and flames were suddenly forced out of the vents in the building. The entire OPE lasted less than 5 s. Firefighters standing adjacent to the street level openings were knocked down and firefighters on the roof reported feeling the roof lift. The overpressure did not cause any noticeable damage to the building and no glass was blown out, nor walls displaced.

On May 8, 2019, the City of Troy (NY) Fire Department was dispatched to a bowling alley fire. The people calling in the incident indicated that black smoke was coming from the roof and the windows of the building. Shortly after arrival, the center of the building was involved in fire from the floor level and venting through the roof. Smoke was banking down to the open street level doors and there was no visibility on the ground floor. The firefighters were pulled out of the building just prior to the OPE that began with high velocity smoke pushing out of the street level doors and extending horizontally 10 to 15 m (30 to 50 ft) out of the building. This phase of the overpressure lasted approximately 20 s before an upstairs window broke out and a high velocity turbulent jet of black smoke flowed out of the window for approximately 12 s before igniting into a horizontal jet flame. Flames also were exiting the ground level doorway. The overpressure behind the jet flames lasted approximately 30 s. After the OPE, a buoyant flame flowed up the building before being blown across the roof of the building by the wind. The horizontal momentum of the flame was replaced by a buoyant plume.

On October 5, 2021, in Portland, OR., the fire department responded to a fire that involved a series of shops and restaurants. The block sized building was originally an auto shop, prior to being sub-divided. When the fire department arrived, the fire had already burned through the roof of the business where the fire started,

and it was spreading into the other shops and restaurants. A master stream was placed into action. Fire had spread to the rear of the restaurant on the corner of the building opposite from the area of origin. The roof of this restaurant was largely intact. Light colored smoke flowed out of many areas of the building just before pressurized smoke, followed by flames, pushed from the rear of the restaurant out, of the front door and horizontally out into the street. Two firefighters in front of the restaurant were knocked down. The OPE lasted less than 10 s.

Between April of 2021 and April of 2023, several residential fires occurred where the fire had extended into the attic space. In one case, the firefighters were venting the roof when the OPE occurred sending jets of heat and smoke up through the roof, down through the house, and out the first-floor doors. In other cases, the firefighters had not vented or changed the ventilation conditions when the OPE occurred.

With regard to the question of "what should these incidents be called?" the incidents generated an overpressure that was enough to knock firefighter down, but not necessarily cause structural damage and often did not even break the glass. The flame fronts evolved in these incidents lasted for a few seconds and were seemingly much slower than a classical deflagration through a flammable air mixture.

All of these incidents shared some common features:

1. Fire was burning for tens of minutes in a void space
2. Void spaces contained significant amounts of fuel with large, exposed surface areas of wood (fuel)
3. Voids were full of smoke and pyrolyzates.
4. In most of the incidents, there was no apparent changes in the ventilation conditions to the void spaces.

This paper does not attempt to fit these events into existing descriptions for backdraft, smoke explosion, hot air explosion, etc. In the context of this paper, the events are simply referred to as overpressure events (OPE) described as the rapid expulsion of combustion products from a building followed immediately by flames that cannot be explained by the accidental release of flammable gases or the ignition of flammable liquids.

Based on the review of the OPEs that occurred in the field, in this research, a series of experiments were conducted in a plywood compartment designed to replicate the common features presented above. The goal of this research is to enhance the understanding of the conditions that lead to an OPE in a combustible compartment with a small wood crib as the ignition source and established fire from a single item. Previous research has investigated the impact of the crib design on smoke explosions [17], but in this project, the crib design was fixed. Also unique to this research, is the use of a single rectangular vent in one of the walls. The rectangular vent is large compared to the previous studies, but the large combustible surface area to vent ratio ensured that the fire was severely ventilation limited. No change in the ventilation opening was made during the experiments. The primary objective for this research is to consistently create an OPE in a com-

bustible compartment so that future research may investigate how to reliably identify the potential for an OPE and develop mitigation strategies for preventing such events from occurring.

2. Experimental Setup

Due to the unexpected nature and unknown severity of an OPE, the experiments were conducted in the open environment outside the laboratory. Experiments were conducted in a small-scale compartment with internal floor dimensions 0.76 m by 1.2 m and 0.76 m ceiling height. The compartment was constructed from 18 mm thick, 5 ply, APA standard sheathing rated plywood (APA Rated Sheathing 2011). The seams along the surface boundaries were lined with 38 mm by 38 mm timber strips to provide structural stability and to help seal the boundary seams. To further seal the compartment, aluminum adhesive tape was installed over all of the external seams. The only vent from the compartment was a 0.40 m by 0.40 m opening centered in one of the small end walls known as the vent wall. The width of the vent was then controlled with additional pieces of plywood fixed to the outer surface of the vent wall. The vent opening height was fixed at 0.40 m for all of the experiments and the width of the vent was varied from 0.10 m to 0.20 m in 0.025 m increments.

The initial fuel package was a timber crib constructed from 38 mm by 38 mm by 200 mm timber sticks. The crib was assembled with three sticks per layer and was five layers in height. The crib weighed 1.8 kg and had an average moisture content between 7 to 9%. The crib was ignited by placing four paper towels (23 g) soaked with 20 g of mineral spirits. The ignition source was sufficient to ignite the crib and burned for approximately 60 s. Within 2 min of ignition, the flames from the crib were impinging on the ceiling. The same crib design was used for all of the experiments. Figure 1 is a photograph showing the interior of the plywood lined compartment with the crib installed against the crib wall opposite the vent wall. The photo was taken just prior to ignition with the paper towels soaked with mineral spirits placed below the crib. The crib was installed 38 mm off the wall and was raised off the floor by four 38 mm timber cubes placed at each corner of the crib. All the experiments were extinguished before any of the cribs collapsed.

The compartment instrumentation was designed to characterize the conditions in the compartment both before and immediately following an OPE. Measurements included, temperature, compartment pressure, gas species (O_2, CO_2, and CO), compartment mass, and vent velocity. Figure 2 is a sketch of the floor plan for the compartment with the instrumentation and internal camera location indicated on the plan.

The gas temperatures were measured using two arrays of inconel sheathed chromel–alumel (type K) thermocouples (TC), 1.6 mm diameter. Such measurements in fire experiments can have uncertainties on the order of $\pm 20\%$ [18] and a response time of approximately 2 s. Although slower to respond than bare bead TC, the sheathed TC were able to be reused for all the experiments. The two TC arrays were installed through one of the long walls, 0.2 m from the crib wall and

Figure 1. Photograph of the plywood compartment interior showing mineral spirits soaked paper towels below the crib just prior to ignition. For scaling the image, the rear wall of the compartment was 0.76 m high and 0.76 m wide.

0.2 m from the vent wall, as shown in Figure 2. The array of TCs started 95 mm below the ceiling and were vertically spaced 95 mm apart, giving a total of 7 TCs in each array.

The velocity through the vent was measured using two bi-directional probes installed 50 mm below the soffit and 50 mm above the sill. A TC was installed at each of the bi-directional probes for gas density estimates. The differential pressure across each probe was measured using Setra Model 264 pressure transducers, with a range of ± 125 Pa. Velocity measurements using bi-directional probes have been shown to have an expanded uncertainty ranging from $\pm 14\%$ to $\pm 22\%$ for pre-flashover fires with the uncertainty increasing as the velocity and temperature in the flow increase [19].

To characterize the intensity of the event, the compartment pressure was recorded at the floor and ceiling along the center of one of the long walls of the compartment as shown in Figure 2. Because the expected pressure level was unknown, five pressure transducers were used to capture the event while still maintaining the desired fidelity of the measurement. The pressure transducers measurement ranges were ± 25 Pa, ± 125 Pa, ± 250 Pa, ± 625 Pa, ± 2500 Pa. The high pressure port was connected to the inside pressure tap and the low side was exposed to atmospheric pressure outside the compartment. In the initial experiments, the pressure was sampled at 1 Hz which proved too slow to reliably capture the peak pressure. For the final five experiments, the sample rate for the pressure was increased to 5 Hz.

Gas samples were drawn directly out of a compartment which was problematic compared to sampling from an exhaust hood. In an exhaust hood, the compartment gases are diluted by the entrained air which dilutes the moisture and soot
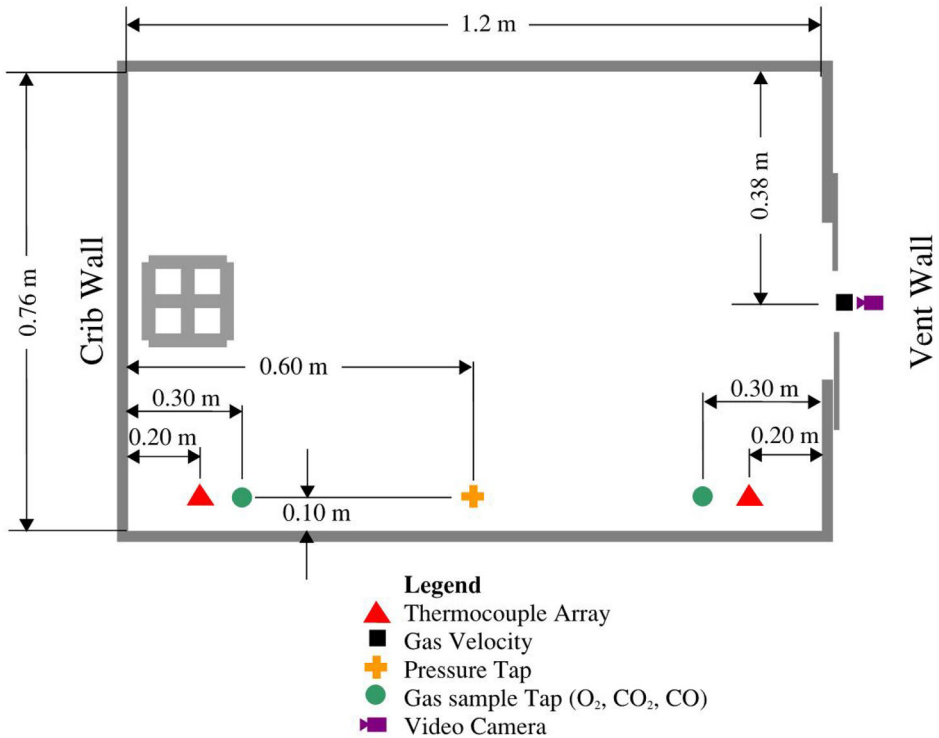
Figure 2. Compartment floor plan showing the instrumentation locations and dimensions.

content in the sample. Both of which must be removed before the sample can be analyzed. In these experiments, under severely limited ventilation, the combustion within the compartment was inefficient by design due to the relatively small size of the vent compared the large fuel surface area of the walls, ceiling, floor, and crib. The severely limited ventilation resulted in large quantities of incomplete combustion products and high moisture content inside the compartment. Typical gas conditioning systems, used for Oxygen Consumption Calorimetry (OCC) would be overloaded as soot filters become clogged and moisture removal systems become saturated. The gas conditioning system was designed to be robust to these conditions, yet the system did clog during some experiments.

Four gas sampling ports were installed in the compartment near the TC arrays as shown in Figure 2. Two sampling ports were located in the upper layer, 0.10 m below the ceiling and two in the lower layer, 0.10 m above the floor. The sample ports were constructed from 9.5 mm stainless steel tubing and once exiting the compartment, the sample was filtered through a Solberg Model 843: 5 micron polyester filter with 0.056 m^2 surface area before being drawn through a condensing coil submerged in an ice bath. Once leaving the condensation coil, the sample was drawn through approximately 20 m of 9.5 mm diameter polyethylene tube.

An additional filter, Solberg model 824: 2 micron with 0.086 m^2 surface area was installed before the Cole Palmer Model L-79200–30 vacuum/pressure diaphragm pump rated at 0.35 lps. The sample was then passed through a desiccant unit to completely dry the sample. To protect the analyzer, the sample was passed through a high efficiency particulate and coalescing filters (Perma Pure Model, 0.01 micron FF-250-E-2.5G filter) designed for high temperature corrosive samples. Ultimately the gas samples were analyzed using Siemens Ultramat/Oxymat analyzers with paramagnetic O_2 analysers and non-dispersive infrared analyzers for the CO and CO_2. The analyzers were calibrated before each experiment from 0 to 25% for the O_2 and CO_2 analyzers and 0–5% for the CO. The gas sampling instruments used for these experiments have demonstrated a relative expanded uncertainty of 1% when compared to span gas volume fractions [20].

A visual record was captured with video cameras at three locations: vent elevation, side wall elevation, and isometric angle to the vent wall. Firefighter infrared (IR) cameras were also included for the elevation views of the vent and side walls. A single camera was installed through the sill below the vent approximately 75 mm above the floor to capture the internal view of the crib and rear wall as shown in Figure 2.

3. Observations

Reviewing the videos from 29 OPE has shown a consistent pattern in the behavior of the compartment fire development over the range of vent widths investigated. This pattern involves four steps and is referred to as a cycle that repeats itself and may culminate in an OPE. The crib fire starts as a typical axisymmetric plume, referred to here as the *axisymmetric plume phase* as seen in Fig. 3A. The image was taken 120 s after ignition, when the flames start to roll across the ceiling. Around 300 s after ignition, the axisymmetric phase gives way to the *detached flame phase* when the flames extend away from the crib in both the horizontal and vertical directions. Figure 3B shows the detached flames around the crib at floor level. After approximately 60 s of detached burning, the flames promptly self-extinguish. Occasionally, some pulsing of smoke can be seen from the vent just before the flames self-extinguishes, and the fire enters into the *smoldering phase*. During the smoldering phase the crib, walls, and ceiling all release pyrolyzates into the compartment. The smoldering phase ends when either the crib reignites, restarting the cycle with a new axisymmetric phase, or the compartment suddenly erupts as an OPE with a horizontally projected flame exiting through the vent. The OPE typically occurs after 2 or 3 cycles. Figure 3A and B are from the initial cycle where the wall and ceiling show only minor charring. Figure 3C is representative of the subsequent axisymmetric phase where the walls have charred and would be expected to contribute to the fuel within the compartment. The subsequent detached phase, also with charred walls and ceiling, is shown in Figure 3D.

Figure 4 is a sequence of video images from the isometric video camera showing the horizontal flame projection that is the culmination of some of the OPEs. The images start approximately 0.5 s after ignition of the OPE that is not visible
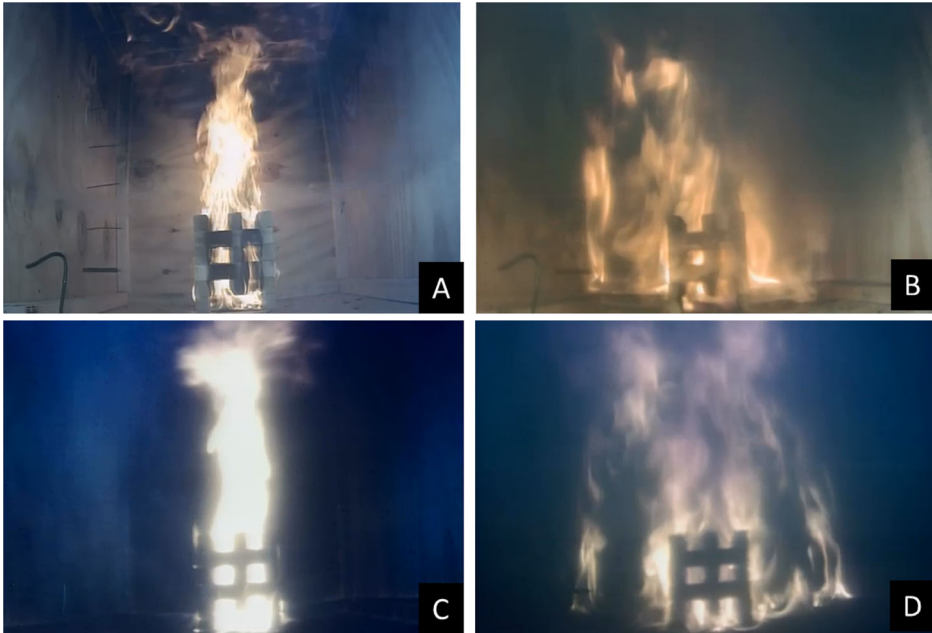
Figure 3. Video images showing significant phases of fire development preceding an overpressure event. For scaling the image, the rear wall of the compartment was 0.76 m high and 0.76 m wide.

from this camera angle. The images are taken 0.1 s apart showing the flame projection and subsequent collapse of the fireball. After an OPE one of two results have been observed, the fire may return to a plume phase and restart the cycle, or the flames may become established in the vent opening, consuming the oxygen at the vent and preventing the cycle from restarting. The final image in Figure 4 shows the flame that has stabilized at the opening and will prevent any further OPE events from occurring. All of the OPEs, from the time of a pressurized flow exiting the compartment to the end of the flow were on the order of one second.

4. Results

The primary objective for this study was to be able to reproduce an OPE within a combustible compartment with similar characteristics to the actual events described in the introduction. A series of 15 experiments were conducted including 3 preliminary runs and 12 subsequent runs with full instrumentation. In the preliminary experiments, it was determined that a 0.4 m high and 0.15 m wide opening was able to repeatably produce an OPE. Often producing multiple events during a single experiment. Subsequent instrumented experiments were conducted varying the width of the opening. In the final five experiments, the scan frequency for the compartment pressure transducer was increased to 5 Hz to better capture any pressure event.

Figure 4. Sequence of video images 0.1 s apart, showing the external horizontal flame projection from an overpressure event from a 0.15 m wide by 0.4 m high vent opening. For scaling the images, the distance from the vent to the edge of the frame is approximately 2.5 m.

Measured conditions prior to each OPE are summarized in Table 1. To maintain consistency in the reported data, the values given in Table 1 were collected 5 s prior to the peak recorded pressure associated with each OPE. In Table 1, each OPE is identified by the experiment number and hyphenated OPE number in that experiment. For example, experiment 4–2 represents the second OPE in experiment 4. The listed times are the time from ignition to peak pressure recorded in the data having first identified the approximate timing of an OPE from the video observations. Species sets for O_2, CO_2, and CO volume fractions are reported for the four locations shown in Figure 2. For some events, the CO readings exceeded the calibrated range of the analyzer (5%), so these values are reported as > 5. The reported temperatures are the top and bottom temperature 4 s before the OPE for each of the 2 TC arrays. The maximum pressure in the compartment is only reported for the 5 Hz results since the 1 Hz was too slow to be meaningful but was able to be used to determine the timing of the event for the data included in Table 1. The average heat release rate (HRR) is estimated from the mass loss measurement of the compartment—the data is inherently crude due to the combustible construction but provides indicative values for comparison. The "Magni-

Table 1
Summary Results Characterizing the Compartments Conditions Prior to all Overpressure Events

Experiment #	Vent Width (mm)	Time (s)	Cycle Number	Crib Wall Upper Layer O2 (vol%)	CO2 (vol%)	CO (vol%)	Crib Wall Lower Layer O2 (vol%)	CO2 (vol%)	CO (vol%)	Vent Wall Upper Layer O2 (vol%)	CO2 (vol%)	CO (vol%)	Vent Wall Lower Layer O2 (vol%)	CO2 (vol%)	CO (vol%)	Crib Wall T Upper (°C)	T Lower (°C)	Vent Wall T Upper (°C)	T Lower (°C)	Pressure 5 Hz (Pa)	HRR (Scale)	Magnitude of event
4-2	150	434	2	14.3	10.6	>5	18.7	3.6	1.9	16.2	5.5	3.3	17.1	7.0	3.5	505	233	429	214		103	3
4-3	150	577	4	4.9	15.3	>5	11.8	9.0	>5	13.8	6.2	2.5	10.8	6.1	2.8	682	361	546	294		103	3
6-2	150	487	2	3.3	14.9	3.0	13.2	6.9	4.0	6.0	11.7	4.6	14.9	2.0	0.9	658	350	550	307		113	3
7-2	150	571	2	8.4	11.7	3.1	13.3	2.4	4.1	6.8	5.7	1.3	13.7	3.7	1.6	624	382	526	332		90	3
11-2	150	1096	5	4.1	7.9	0.9	16.6	2.2	1.1	5.7	8.9	0.9	10.3	4.8	2.3	624	291	516	284	47	86	3
12-1	150	583	3	5.0	12.8	1.2	12.9	6.8	3.8	6.9	7.9	1.4	9.7	10.1	4.5	635	350	492	280	97	88	3
13-1	150	649	3	8.4	8.1	1.4	12.2	7.0	3.6	9.6	6.8	1.5	11.2	10.2	4.3	640	376	503	311	73	92	3
9-1	200	368	3	8.4	11.5	2.5	16.0	5.1	3.9	9.7	11.9	>5	17.7	1.2	0.7	549	296	470	268		117	2
9-2	200	403	4	7.0	11.7	1.7	14.0	4.1	2.8	5.4	13.2	4.0	17.6	1.6	0.6	703	366	555	297		117	2
6-3	150	826	3	4.1	12.9	0.8	7.7	14.3	5.2	6.2	11.8	2.6	11.4	6.4	3.0	634	492	539	343		113	2
8-1	150	516	2	11.0	8.1	1.5	14.9	1.4	1.4	1.0	15.7	3.6	11.4	1.1	0.6	657	302	529	285		100	2
14-4	175	543	4	0.5	18.0	>5	13.0	5.8	4.2	3.5	15.7	>5	12.3	8.6	4.9	645	353	504	294	143	100	2
5-2	100	1168	4	*	*	*	15.2	6.5	4.6	9.7	10.4	5.3	13.7	7.7	5.2	490	328	438	268		57	2
15-4	100	1071	4	14.5	6.9	3.6	17.0	4.1	2.1	14.1	5.8	3.2	15.9	3.8	2.3	458	335	478	335	121	66	2
7-1	150	399	1	16.5	4.8	3.1	19.5	3.6	0.7	11.4	9.7	5.2	19.2	2.9	2.3	451	220	390	195		90	1
5-1	100	1088	2	*	*	*	18.0	3.7	1.8	12.0	8.9	5.1	16.9	5.2	2.8	414	221	377	196		57	1
15-3	100	1002	3	14.2	6.8	3.5	18.9	2.4	1.2	13.6	5.9	3.1	17.8	2.6	1.5	440	241	450	249	132	66	1
15-5	100	1159	5	14.2	5.4	2.3	18.9	2.4	1.0	14.7	4.7	2.2	18.5	2.3	1.1	394	247	441	232	126	66	1
15-6	100	1212	6	15.2	11.6	>5	12.5	8.4	>5	7.6	9.7	>5	12.3	7.5	>5	601	379	499	328	84	66	1
10-1	175	391	1	0.7	16.4	>5	8.2	10.3	>5	0.2	15.3	>5	12.6	6.2	>5	663	664	555	379		126	0
14-1	175	405	1	8.5	16.3	>5	15.2	8.3	3.7	8.6	14.0	>5	14.4	11.0	>5	514	311	443	280	49	100	0
14-2	175	443	2	9.0	16.4	>5	16.0	6.0	2.9	10.4	13.7	>5	16.3	7.6	3.1	524	292	442	260	45	100	0
14-3	175	499	3	14.5	7.1	3.6	19.6	2.9	0.9	14.6	6.5	3.2	19.6	3.5	1.4	405	234	360	207	16	100	0
4-1	150	373	1	13.3	7.3	3.4	20.3	1.1	0.4	17.6	3.7	1.8	19.8	2.0	1.3	415	172	374	170		103	0
6-1	150	441	1	13.4	9.7	>5	19.6	1.6	1.0	12.4	7.8	5.2	18.6	3.4	2.8	459	238	427	219		2	0
11-1	125	826	3	0.6	17.7	>5	13.1	6.6	3.1	0.4	17.6	>5	5.5	12.2	>5	655	474	538	337	35	86	0
5-3	100	1196	5	*	*	*	12.0	10.6	4.1	6.0	12.4	5.2	11.4	7.3	3.9	612	386	496	301		57	0
15-1	100	768	1	16.9	3.7	1.9	19.7	1.3	0.6	17.1	3.0	1.8	19.5	1.1	0.6	253	132	231	109	29	66	0
15-2	100	908	2	14.6	6.6	3.4	19.1	2.0	1.0	13.8	5.4	2.6	19.0	1.9	1.1	449	235	445	208	124	66	0
AVG				9.4	10.7	**	15.4	5.2	**	9.5	9.5	**	14.8	5.2	**	543	319	467	268	80	86	
MAX				16.9	18.0	3.6	20.3	14.3	5.2	17.6	17.6	5.3	19.8	12.2	5.2	703	664	555	379	143	126	
MIN				0.5	3.7	0.8	7.7	1.1	0.4	0.2	3.0	0.9	5.5	1.1	0.6	253	132	231	109	16	2	
Standard Deviation				5.3	4.3	1.0	3.5	3.3	1.5	4.9	4.0	1.5	3.7	3.3	1.4	114	106	73	60	44	26	

* - Measurement not reported, sample line was blocked.

** - In some of the experiments the CO measurement exceeded 5% (exceeds range of analyzer) so the average value is not reported.

tude of event" is a relative measure of the horizontal flame extension out of the compartment vent. A value of 3 indicates a flame extending over 2 m from the vent (rows in blue), 2 indicates flames extending 1–2 m (rows in orange), 1 indicates the flames extending up to 1 m from the vent (rows in green), and 0 indicates no visible flame out of the vent (rows with no color). The OPE shown in the sequence of video images in Fig. 4 is a flame extension of magnitude 3. The data in Table 1 has been arranged with the greatest flame extension, i.e. 3, at the top and diminishing down the table. Secondary sorting criteria was the vent opening width.

The cycle number given in Table 1 points out that even if an OPE is listed as "-1" in a given experiment, that OPE may have occurred after two to four cycles. A cycle includes the cessation of flaming combustion in the compartment and then the re-start of flaming combustion in the compartment. This cycling results in an oscillating flow at the vent opening. Some cycles result in a slight pulse of smoke out of the vent, in other cases it results in an OPE. In the configuration used in this series of experiments, the 150 mm wide vent generated most of the higher magnitude OPEs. In the case of experiment 11–2, the experiment started with a vent width of 125 mm. After three cycles, OPE 11–1 occurred with a magnitude 0 OPE. Another cycle occurred with no event. The vent width was adjusted to 150 mm and an OPE with a magnitude of 3 occurred on the next cycle.

The four rows included at the bottom of Table 1 provide the average, maximum, minimum, and standard deviation of the results. The results for the O_2 concentration in the upper layer shows that the average value in the upper layer was 9.4% near the crib wall and 9.5% near the vent wall. In the lower layer, the average concentration was much higher at 15.4% near the crib and 14.8% near the vent. Considering these results in the context of ignition of the OPE, the limiting O_2 concentration (LOC) for plywood pyrolyzates under anaerobic conditions have been experimentally measured to be 9% at 20 ℃, see ref [21]. Research on the LOC [22, 23] at elevated temperatures shows that the LOC decreases with elevated temperatures. This indicates that in most of the experiments, ignition of an OPE is possible in both the lower and upper layers. However, the higher oxygen concentration in lower layer indicates that the ignition is expected to be easier in the lower layer. In many experiments, it was difficult to see the ignition location in the compartment from the exterior cameras. Even the internal camera was often blurred by the smoke making it difficult to accurately discern the location of the ignition. In some cases, the ignition location could be identified as a small white spot in an otherwise dark single video frame. There was not a consistent ignition location; ignition was observed within the crib, directly above the crib and high above the crib in the layer near the ceiling.

The CO concentration is more commonly of interest as a toxic product, however in this study the CO is of more interest as a contributor to the flammability of the compartment gases and an indicator of incomplete combustion. As previously mentioned, in some of the experiments the CO analyzer became saturated above 5%. With this limitation, the average CO concentrations are not reported. The CO concentrations are considered to be Immediately Dangerous to Life or Health (IDLH), yet they are below the lower flammable limit of 12.5% at STP

[24]. This indicates that when an OPE occurs, there must be significant quantities of flammable gases that were not able to be measured in this study. Previous research [16] on smoke explosions have demonstrated that the CO concentration alone is not sufficient to produce a flammable mixture in the compartment.

4.1. Heat Release Rate Data

The heat release rate from a timber crib in a non-combustible compartment is governed by one of three conditions: the surface area of crib, crib porosity, or the ventilation limit for the compartment. The surface area and the porosity control are a function of the geometry of the crib and are described in ref [25]. Ventilation limit of the pyrolysis rate for a timber crib in a noncombustible compartment is a function of the size of the opening using the well-known relationship [25]:

$$\dot{m}_p = 0.12 A_o \sqrt{H_o} \tag{1}$$

where:

$\dot{m}_p -$ crib pyrolysis rate $\left(\dfrac{\text{kg}}{\text{s}}\right)$

$A_o -$ area of the opening (m^2)

$H_o -$ height of the opening (m)

Equation 2 is an enhancement on the stoichiometric pyrolysis rate for a compartment derived from the air flow rate into the compartment that can be written as [25]:

$$\dot{m}_p^{Stoich} = \frac{0.5}{r} A_o \sqrt{H_o} \tag{2}$$

where:

$\dot{m}_p^{Stoich} -$ stoichiometric crib pyrolysis rate based on the amount of air

entering the compartment $\left(\dfrac{\text{kg}}{\text{s}}\right)$

$r -$ stoichiometric air/fuel mass ratio, in this study for timber, $r = 5.7$.

Dividing $\dot{m}_p = 0.12 A_o \sqrt{H_o}$ Eq. 1 by $\dot{m}_p^{Stoich} = \frac{0.5}{r} A_o \sqrt{H_o}$ Eq. 2 shows that the pyrolysis rate for a timber crib in a ventilation limited compartment is a 37% increase in the pyrolysis rate over the stoichiometric pyrolysis rate, thus the compartment is considered to be fuel rich.

Table 2 shows the three control conditions for a timber crib in a compartment and the calculated HRR for each. The HRR is calculated by multiplying the pyrolysis rate by the assumed heat of combustion (ΔH_c) for timber, 12000 MJ/kg [25]. The surface area control is a function of time and is a maximum at $t = 0$. Two surface area control values are given in Table 2, the maximum HRR

Table 2
Heat Release Rate for the Timber Crib in Compartment Based on the Surface Area Control, Porosity Control, and Ventilation Control

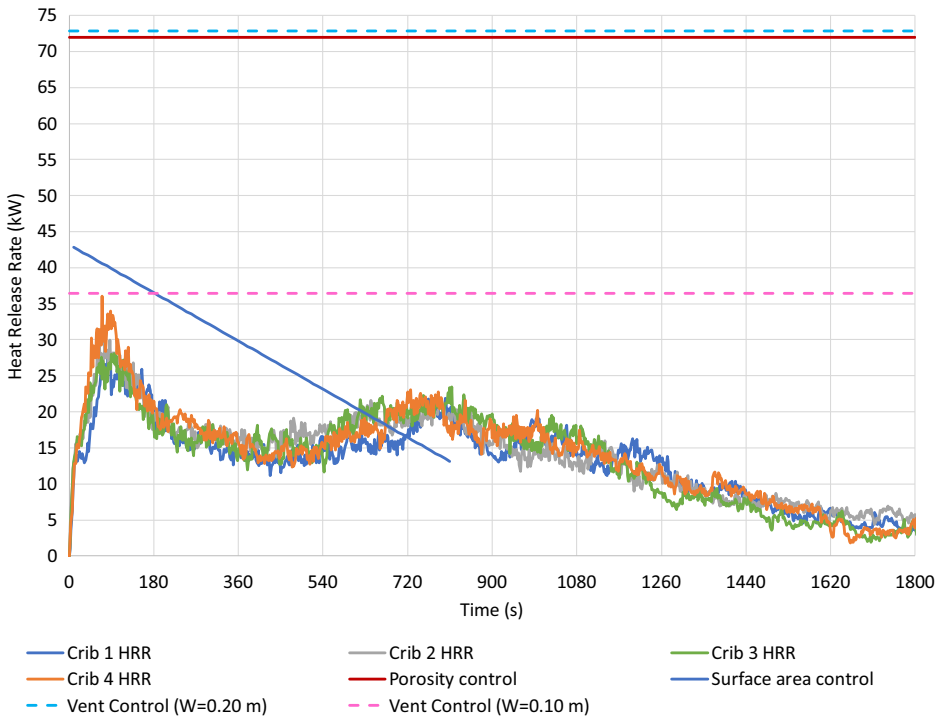| Control on heat release rate	Heat release rate (kW)
Surface area control at $t = 0$	43
Surface area control at $t = 810$ s (crib is 90% consumed)	13
Porosity control	72
Compartment ventilation control ($w = 0.2$ m)	73
Compartment ventilation control ($w = 0.1$ m)	36

Figure 5. Heat release rate history from the calorimetry tests for four identical cribs used in the overpressure event experiments.

(43 kW) at t = 0 s and 19 kW after 90% of the crib mass would be consumed (t = 810 s). After 810 s, it is assumed the crib would collapse and be reaching burnout so the correlation may not apply. Two ventilation control values are given based on the limits on the opening width (0.1 m≤w≤0.2 m). For the 0.2 m wide vent the ventilation-controlled heat release rate is 73 kW and for the 0.1 m wide vent the ventilation-controlled heat release rate is 36 kW.

To determine the actual HRR for the crib used in the experiments, four replicate calorimetry tests were conducted on identical cribs. Figure 5 shows the HRR

Table 3
Heat Release Rate for the Ventilation-controlled Burning (Equations 1 and 2) Compared to the Experimental Heat Release Rate Based on the Compartment Mass Loss Rate Times the Heat of Combustion

Opening width (m)	$A_o \sqrt{H_o}$ m$^{(5/2)}$	HRR for ventilation controlled combustion in compartments (Equation 1 ΔHc)	HRR for stoichiometric combustion in compartments (Equation 2 ΔHc) (kW)	HRR experimental average mass loss rate times ΔHc (kW)	φ-Global equivalence ratio (Calculated)
0.100	0.0253	36	27	62	2.3
0.125	0.0316	46	33	86	2.6
0.150	0.0379	55	40	97	2.4
0.175	0.0443	64	47	113	2.4
0.200	0.0506	73	53	117	2.2

history for the four replicate test results along with the calculated surface area, porosity and ventilation-controlled values. The results show how consistent the HRR from the timber cribs are. The calculated controls on the HRR show that for the 0.10 m wide vent, the fire would be ventilation-controlled for the first 180 s. After this time, the fire would become controlled by the surface area. For larger vent widths used in this study, the fire would be controlled by the surface area. It should also be noted that the heat release rate for the crib alone would not be controlled by the ventilation into the compartment.

The above discussion only quantifies the item first ignited, i.e. the crib. Estimating the contribution from the combustible compartment is more difficult. Because the experiments were conducted outside in the open atmosphere, HRR calorimetry was not available. In addition, the combustible construction meant that it was not possible to isolate the fuel sources on a load cell as done in previous smoke explosion research in non-combustible compartments [14–16]. It was, therefore, necessary to place the entire compartment on a load cell platform to obtain a continuous measurement of the compartment mass. These results provide an estimate of the mass loss rate for the crib plus all of the mass loss from the compartment surfaces. Measuring the entire compartment is hampered by the buoyancy of the hot gas layer, drag on instrumentation cabling and sample lines, along with the impact of any ambient wind conditions. Although not an ideal measurement, given the experimental constraints, there was no other method available for estimating the HRR or mass loss rate in these experiments.

Table 3 compares the calculated and measured HRR values for the vent widths used in these experiments. Column 1 gives the width of the vents used in the experiments (0.1–0.2 m). Column 2 is the opening factor $\left(A_O\sqrt{H_O}\right)$ using the vent width and 0.4 m height. Columns 3 & 4 give the calculated HRR for ventilation-controlled combustion and the calculated stoichiometric HRR for the compartment using Equations 1 and 2, respectively. Column 5 gives the experimental HRR calculated from the compartment mass loss rate times the heat of combustion of 12,000 kJ/gm. Dividing the experimental HRR (column 5) by the HRR for
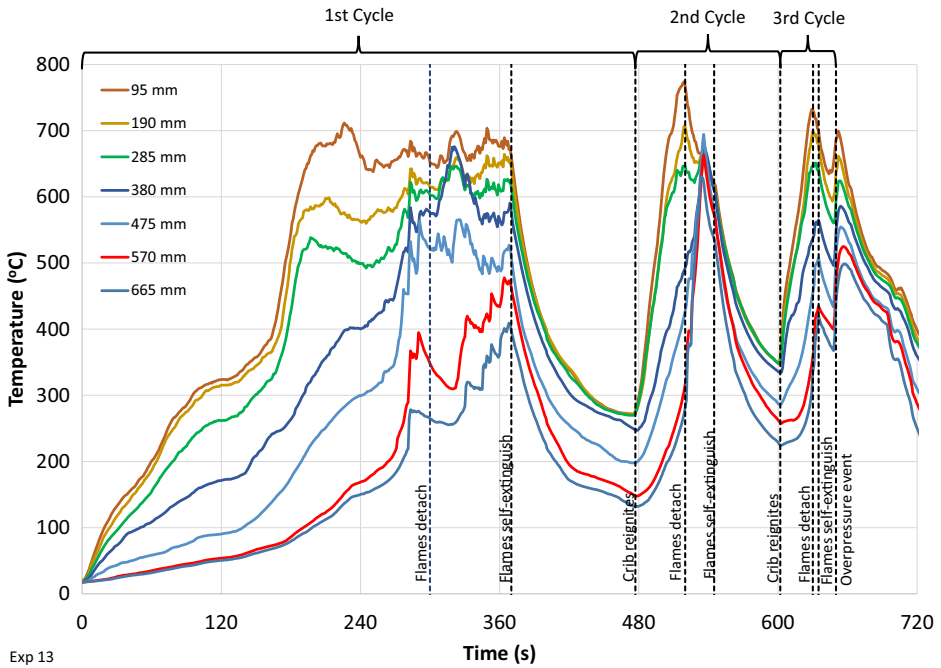
Figure 6. Exemplar temperature history for the thermocouple array near the crib wall highlighting the three cycles of reignition, detached flaming, and self-extinguishment culminating the ignition of an overpressure event..

stoichiometric combustion in the compartment (column 4) provides an estimate of the global equivalence ratio for the compartment that is shown in column 6. The global equivalence ranges from 2.2 to 2.6 which demonstrates that the conditions in the compartment are fuel rich.

4.2. Temperature Data

Figure 6 shows the temperature histories from the thermocouple array near the crib wall of the compartment for experiment 13 where there was only one OPE. Several noteworthy events in the experiment are shown along the timeline. Highlighted on the temperature history plot is the crib reignition, detached flaming, and self-extinguishment for 3 cycles. In experiment 13, the only OPE occurred at 649 s, at the end of the 3rd cycle. The first cycle starts with the ignition of the mineral spirits-soaked paper towels under the crib at time 0. The crib fire becomes established quickly from this strong ignition source. After 3 min, the top three TCs exceed 500 ℃ in the compartment. The top three TCs then start to plateau while the temperature of the lower TCs continue to rise. When the flames detach from the crib and start to travel around the compartment, only the temperature of the bottom two TCs continue to increase while the upper TCs continue to pla-

Exp 13

Exp 13
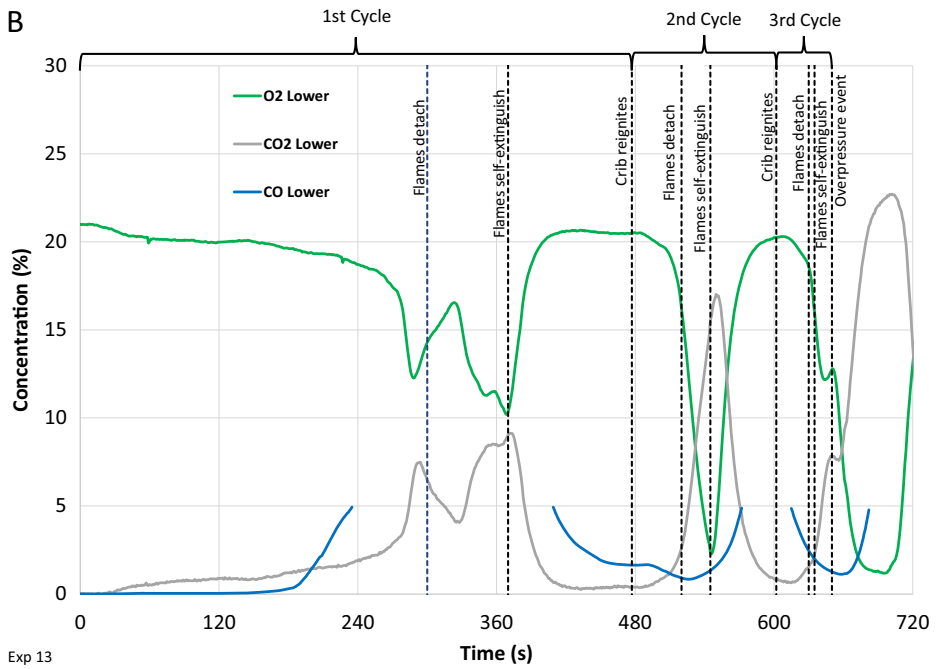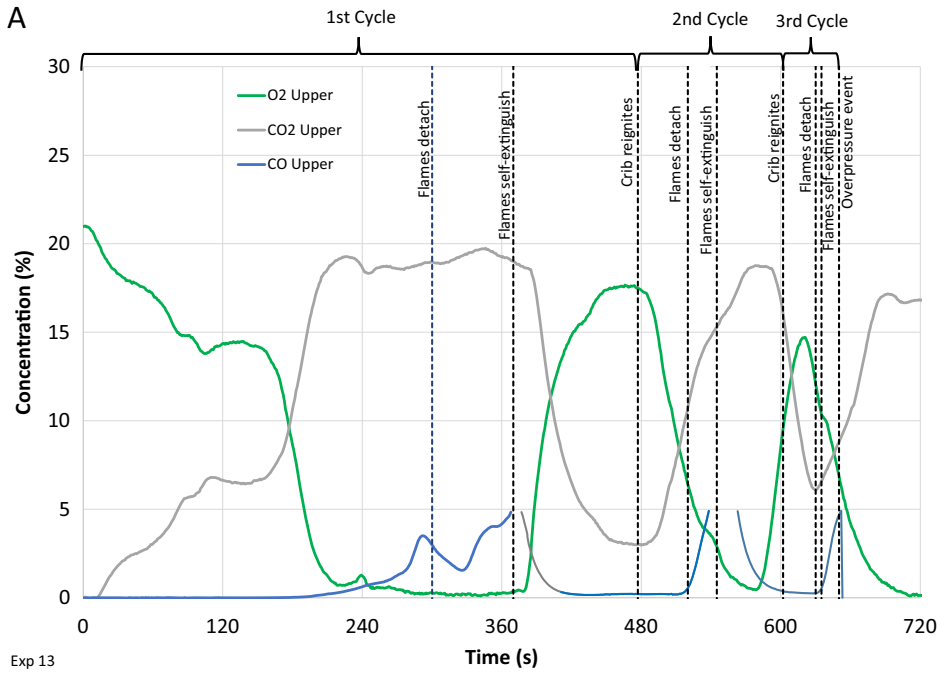
◄**Figure 7. (A) and (B) Exemplar gas species history from experiment 13 shows the three cycles of reignition, detached flaming, and self-extinguishment culminating with the ignition of an overpressure event after three cycles. (A) shows the crib side upper layer analyzers and (B) is the crib side lower layer analyzers. Note: where the CO concentration exceeds the range of the analyzer (5%) the data is truncated.**

teau. By 370 s, the flames self-extinguish and the temperatures of all the TCs start to decay exponentially until the crib reignited at 475 s. After reignition, the second cycle begins but lacks the long plateau period seen in the first cycle and the cycle is much shorter in duration. The second cycle also ends when the crib reignites, starting the third cycle. The third cycle exhibits the same three phases identified in previous two cycles. Each successive cycle was noticeably shorter, 480 s for the first, 120 s for the second, and 50 s for the third. This experiment was ended after the OPE, when the flames became established at the vent. Once the flame becomes established at the vent, air is prevented from entering the compartment and the unburned fuel released in the compartment is consumed in the external flame (as seen in the last three frames of Figure 4).

4.3. *Species Data*

Exemplar species history from experiment 13 for the samples near the crib wall for both the upper (A) and lower (B) layers are shown in Figure 7 A and B. The same cyclic behavior described in Figure 6 is also seen in Figure 7. Note: where the CO concentration exceeds the range of the analyzer (5%) the data is truncated. The combustion of the crib quickly reduces the O_2 concentration in the upper layer while simultaneously CO_2 accumulates in the upper layer. Around 150 s the fire starts to become limited by the ventilation as the CO concentration increases. By 220 s, the O_2 concentration in the upper layer is nearly consumed yet in the lower layer the O_2 is still quite high at 19%. Around 300 s the flames become detached and moves around the compartment. As the detached flames travel around the compartment, the O_2 in the lower layer starts decreasing and the detached flame starts to run out of O_2. By 370 s, the detached flames self-extinguish, and the timber starts to smolder. With only smoldering combustion in the compartment, O_2 starts to increase, the CO_2 and CO concentrations decline until the O_2 reaches a level that the crib reignites. This cycle repeats itself but each time the cycle repeats, the duration of the cycle reduces.

4.4. *Velocity*

The vent flow velocity was measured with two bi-directional probes capturing the flow into and out of the compartment. A positive velocity, indicates flow out of the compartment, typical of the flow out of the top of the vent. Negative velocity, demonstrates a flow into the compartment, commonly associated with the flow into the bottom of the opening. During the experiments, as the oxygen level drops, the flame on the crib will start to pulse before becoming detached from the crib and

moving around the compartment. This pulsing behavior causes the flow in the vent to momentarily transition from bi-directional to unidirectional making the vent flow unstable. This can be seen in the velocity measurements, especially for the bottom probe when the velocity becomes momentarily positive, indicating that the lower flow of the vent is out of the compartment. As the pulsing behavior becomes more frequent, the flame will detach from the crib and move around the compartment. This can be seen in Figure 8 as the positive spikes in the bottom probe data become more frequent. These short duration pulses are on the order of seconds and are not accurately captured with the 1 Hz scan rate used in these experiments. This highly transient vent flow also makes it challenging to interpret the mass flow calculations during this behavior and in the vicinity of the OPE. With little confidence in the mass flow calculations during these cycles, estimates of the equivalence ratio near the OPE were considered too unreliable to report in this paper.

4.5. Pressure Data

Figure 9 shows the pressure history from the 5 Hz scan rate zooming in on the last cycle before the OPE in experiment 13 (59009 s<t<670 s). The crib reignites at 602 s and there is a slight increase in the compartment pressure. The fire then burns as an axisymmetric plume (Figure 3C) for approximately 30 s. The flames then detach from the crib and burn around the crib before self-extinguishing 7 s later. During the detached flaming phase, pulsing can be seen in the pressure history. Once the flames self-extinguishes, the compartment continues to pyrolyze but there is insufficient O_2 to burn. After 13 s of no visible flame, the OPE ignites sending a long horizontal flame out through the vent and spiking the compartment pressure over 175 Pa. At the 5 Hz scan frequency, the pressure spike is just 4 scans, 0.8 s in duration. After the OPE, the flame become established in the opening and the experiment is terminated.

5. Conclusions

Based on the review of the OPEs that occurred in the field, the compartment was built with a wood interior finish.

The results of this research identified a consistent cycle in a combustible compartment that precedes an OPE and, in many cases, multiple OPEs in the same experiment. The cycle consists of three phases:

1. axisymmetric plume phase
2. detached flaming phase
3. smoldering phase

The axisymmetric plume phase starts with the flaming ignition or reignition of the crib. The detached flaming phase starts when the flames expand away from the crib in both the horizontal and vertical directions. The smoldering phase starts when the detached flame self-extinguishes. The smoldering phase ends with the ignition of an OPE, or the reignition of the crib as an axisymmetric plume restart-
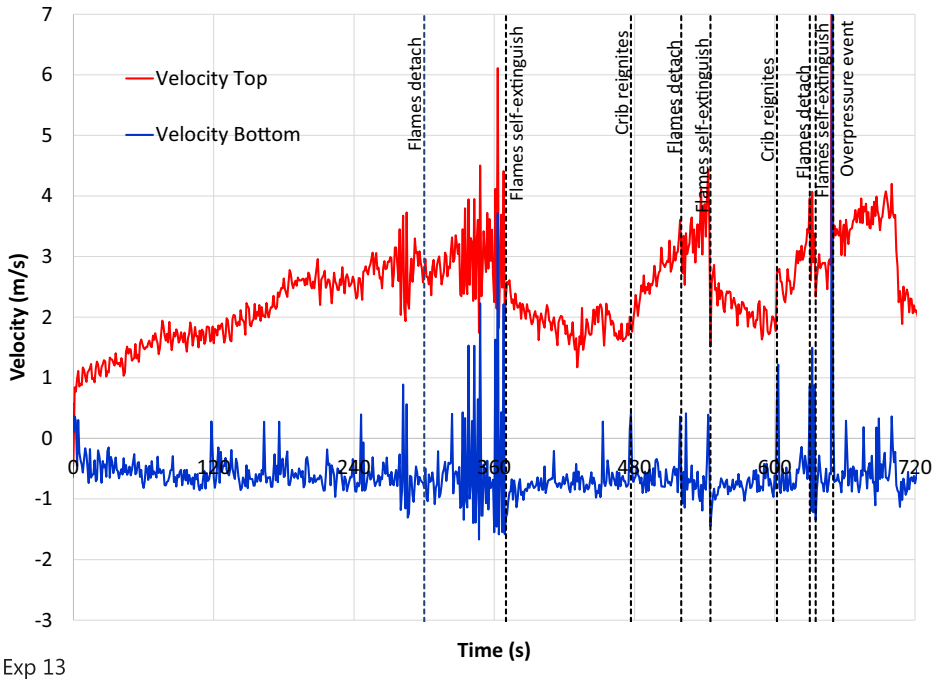
Exp 13

Figure 8. Vent flow velocity history for the two bi-directional probes placed 50 mm below the soffit and 50 mm above the sill.

ing the cycle. These three phases are collectively referred to as a cycle and may repeat multiple times before an OPE occurs. When multiple cycles occur before an OPE, the duration of each successive cycle is reduced.

This cycle was observed for all of the vent opening widths and the duration of each phase increased as the vent opening width decreased.

Although the CO concentrations were IDLH, the values were below the flammable range indicating that there must be other flammable products from the wood pyrolysis that contribute to the occurrence of an OPE.

The following observations for the fire service to look for are based on the examinations of actual commercial and residential scale OPE events and these experiments:

- The potential for an OPE is increased once the fire has spread to where large surface areas of smoldering fuel, such as wood, are involved
- Ventilation limited compartments, such as attics or void spaces, increase the potential for an OPE
- Oscillating flows out of openings may be a pre-cursor to an OPE
- The OPE can occur without any change in ventilation
- Multiple OPEs may occur in the same area if no action is taken to change the conditions
- Effective application of water into the compartment can prevent an OPE
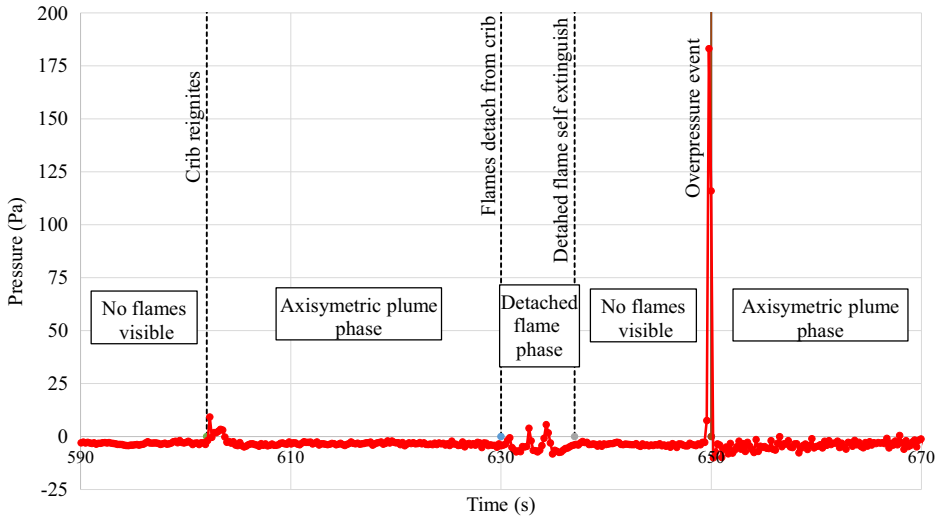
Figure 9. **Detailed pressure profile covering 80 s including the final cycle (reignition, axisymmetric plume, detached flaming, self-extinguishment, and reignition) culminating in an overpressure event.**

- Increasing ventilation may be the catalyst (or trigger) for an OPE.

6. Future Research

- Vent opening height and width should be investigated to determine the range of vent opening factors that can result in an OPE.
- Pressure measurement frequency should be increased, and the transducer response improved to 100 Hz to better characterize the pressure profile of the OPE and the vent velocity measurement.
- Total hydrocarbon concentration or phi measurements should be added during each experiment to further evaluate the flammability in the compartment gases.
- The calibrated range for the CO concentration should be increased to 10% to capture the peak concentrations.
- Experiments should be conducted inside a laboratory to reduce the impact of the local environment and allow for oxygen consumption calorimetry measurements.
- Future experiments should explore the use of laser diagnostics to better understand the flow field and the details of the species concentrations.
- Once the OPEs are better understood, examine firefighting tactics and tools which can interfere with the fire dynamics and prevent the OPEs.

Acknowledgements

Open Access

References

1. Steward PDC (1914) Dust and smoke explosions. Nat Fire Prot Assoc Q 7:424–428
2. Croft WM (1980) Fires involving explosions - A literature review. Fire Saf J 2:3–24. https://doi.org/10.1016/0379-7112(80)90003-X
3. Chitty R (1994) A Survey of Backdraught, Fire Research Station, Home Office – Fire Research and Development Group, London, https://www.ukfrs.com/sites/default/files/2017-09/Publication%205_94%20-%20A%20Survey%20of%20Backdraught.pdf
4. Fahy RF (2020) U.S. Fire Service Fatalities at Structure Fires: 1977–2018, National Fire Protection Association, 2020. https://www.nfpa.org/-/media/Files/News-and-Research/Fire-statistics-and-reports/Emergency-responders/OSTrendsFFDeathsStructureFires.ashx, Accessed 31 Jan 2023
5. NFPA 921 (2021) Guide for Fire and Explosion Investigations, National Fire Protection Association
6. Fleischmann CM, Chen ZJ (2013) Defining the difference between backdraft and smoke explosions. Proceedia Eng 62:324–330. https://doi.org/10.1016/j.proeng.2013.08.071

7. Gottuk DT et al (1999) Development and Mitigation of backdraft: a real-scale shipboard study. Fire Saf J 33(4):261–282. https://doi.org/10.1016/S0379-7112(99)00033-8

8. Guigay G et al (2010) 2010 The influence of thermal instabilities on the initial conditions of the backdraft phenomenon. Combust Sci Technol 182:4–6. https://doi.org/10.1080/00102200903504176

9. Ferraris SA, Wen JX, Dembele S (2008) Large Eddy simulation of the backdraft phenomenon. Fire Saf J 43(3):205–225. https://doi.org/10.1016/j.firesaf.2007.06.009

10. Wu Cl, Santamaria S, Carvel R (2020) Critical factors determining the onset of backdraft using solid fuels. Fire Technol 56:937–957. https://doi.org/10.1007/s10694-019-00914-9

11. Weng WG, Fan WC (2003) Critical condition of backdraft in compartment fires: a reduced-scale experimental study. J Loss Prev Process Ind 16:19–26. https://doi.org/10.1016/S0950-4230(02)00088-8

12. Wu CL, Carvel R (2017) An experimental study on backdraught: the dependence on temperature. Fire Saf J 91:320–326. https://doi.org/10.1016/j.firesaf.2017.04.003

13. Flakenstein-Smith R, Cleary T (2023) Gas mixture conditions conducive to backdraft phenomenon. Fire Saf J 141. https://doi.org/10.1016/j.firesaf.2023.103998

14. Sutherland BJ (1999) Smoke Explosions, in Civil and Natural Resources Engineering, University of Canterbury. https://ir.canterbury.ac.nz/handle/10092/8328

15. Chen ZJN (2012) Smoke Explosion in Severally Ventilation Limited Compartment Fires, University of Canterbury, https://ir.canterbury.ac.nz/handle/10092/7830

16. Rasoulipour S (2022) Experimental investigation of the smoke explosion phenomenon, PhD Thesis, University of Canterbury, https://ir.canterbury.ac.nz/handle/10092/103797

17. Rasoulipour S, Fleischmann C (2023) Experimental investigation of the smoke explosion phenomenon. Fire Saf J . https://doi.org/10.1016/j.firesaf.2023.103881

18. Blevins LG (1999) Behavior of bare and aspirated thermocouples in compartment fires. In: National Heat Transfer Conference, 33rd Proceedings, p 15–17

19. Bryant RA (2009) A comparison of gas velocity measurements in a full-scale enclosure fire. Fire Saf J 44:793–800. https://doi.org/10.1016/j.firesaf.2009.03.010

20. Bundy M, Hamins A, Johnsson EL, Kim SC, Ko GH, Lenhart DV (2007) Measurements of Heat and Combustion Products in Reduced-Scale Ventilated-Limited Compartment Fires. NIST Technical Note 1483, National Institute of Standards and Technology, Gaithersburg, MD.

21. Rasoulipour S, Fleischmann C, Mercieca L, Adams N (2022) Flammability of engineer wood pyrolysis gases at anaerobic conditions". Fire Saf J . 10.1016/j.firesaf.2021.103424

22. Razus D, Molnarne M, Movileanu C, Irimia A (2006) Estimation of LOC (limiting oxygen concentration) of fuel–air–inert mixtures at elevated temperatures by means of adiabatic flame temperatures. Energy 45(3):193–197. https://doi.org/10.1016/j.cep.2005.06.010

23. Li P, Liu Z, Li M, Zhao Y, Li X, Wan S, Ma Y, He Y (2020) Investigation on the limiting oxygen concentration of combustible gas at high pressures and temperatures during oil recovery process. Energy. https://doi.org/10.1016/j.energy.2020.119157

24. Beyler C (2016) Flammability limits of premixed and diffusion flames. SFPE Handb Fire Prot Eng. https://doi.org/10.1007/978-1-4939-2565-0

25. Babrauskas V (2016) Heat release rate. SFPE Handb Fire Prot Eng. https://doi.org/10.1007/978-1-4939-2565-0